Cell Reports
Physical Science

CellPress
OPEN ACCESS

Review

Light-Emitting Probes for Labeling Peptides

Andreia Boaro,[1,2] Lucía Ageitos,[1,3] Marcelo Torres,[1] Fernando Heering Bartoloni,[2,*] and Cesar de la Fuente-Nunez[1,*]

SUMMARY

Peptides are versatile biopolymers composed of 2–100 amino acid residues that present a wide range of biological functions and constitute potential therapies for numerous diseases, partly due to their ability to penetrate cell membranes. However, their mechanisms of action have not been fully elucidated due to the lack of appropriate tools. Existing light-emitting probes are limited by their cytotoxicity and large size, which can alter peptide structure and function. Here, we describe the available fluorescent, bioluminescent, and chemiluminescent probes for labeling peptides, with a focus on minimalistic options.

INTRODUCTION

Peptides display numerous biological activities, including antimicrobial, immunomodulatory, analgesic, anti-inflammatory, antioxidant, and anticancer properties.[1,2] Depending on their physicochemical properties, peptides can attack the physical integrity of cellular membranes through different modes of action and/or translocate into the cell, interfering with intracellular targets and eventually blocking biological processes vital to the cell.[3] However, the multifunctional mechanisms of action (MoA) of peptides are not entirely understood. Fluorescent and luminescent methods can help elucidate the MoA of these molecules (Figure 1A), but the lack of suitable fluorescent probes, mainly due to their large size and toxicity, has traditionally limited this area of research. In this review, we provide an overview of recently described fluorescent and luminescent probes that may help elucidate the MoA of antimicrobial peptides (AMPs) specifically, and peptides more broadly.

Fluorescence Imaging

Non-natural Fluorescent Amino Acids (FlAAs)

Amino acid residues, such as tryptophan (Trp), tyrosine, and phenylalanine, are intrinsically fluorescent due to their aromatic side chain groups (Table 1).[4] Trp is the most commonly used amino acid for this purpose and has been used as a fluorescent probe for labeling peptides and studying protein folding.[5] However, the spectroscopic properties of Trp are complex, due to its multi-exponential fluorescence decay with two different lifetimes ($t_{1/2}$, Table 1), caused by the emission from two nearly identical electronic transitions.[6] Efforts have been made to try to modify the chemical structure of natural FlAAs to improve their fluorescent properties (i.e., fluorescent quantum yield [Φ_{FL}], $t_{1/2}$, and Stokes shift).[4] Φ_{FL} can be defined as the ratio between the number of molecules that undergo radioactive decay from the excited singlet state (S_1) to the ground state (S_0) and the total number of molecules that are excited to S_1 by photon absorption.[7] Light-emitting probes display significant changes in their spectroscopic properties when exposed to environments with different polarity. When a fluorescent probe interacts with the cell membrane, its fluorescence emission intensity increases, and a hypsochromic shift of the

[1]Machine Biology Group, Departments of Psychiatry and Microbiology, Institute for Biomedical Informatics, Institute for Translational Medicine and Therapeutics, Perelman School of Medicine, and Department of Bioengineering, University of Pennsylvania, 3610 Hamilton Walk, Philadelphia, PA 19104, USA

[2]Centro de Ciências Naturais e Humanas, Universidade Federal do ABC, Avenida dos Estados, 5001, Santo André, São Paulo 09210-580, Brazil

[3]Centro de Investigacións Científicas Avanzadas (CICA) e Departamento de Química, Facultade de Ciencias, Universidade da Coruña, Calle de la Maestranza, 9, A Coruña 15071, Spain

*Correspondence: fernando.bartoloni@ufabc.edu.br (F.H.B.), cfuente@pennmedicine.upenn.edu (C.d.l.F.-N.)

https://doi.org/10.1016/j.xcrp.2020.100257

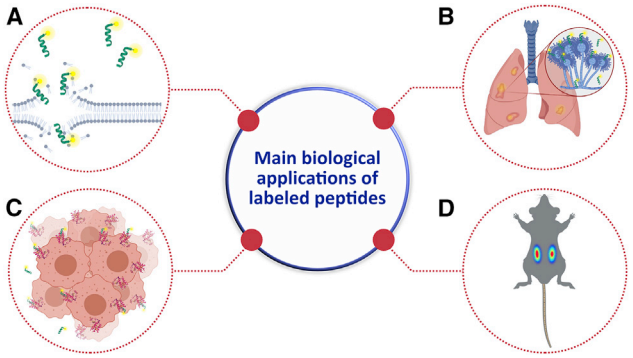

Figure 1. Biomedical Applications of Peptides Labeled with Light-Emitting Probes

(A) Study of the mechanisms of action of antimicrobial peptides.

(B) Tracking of infections (e.g., invasive pulmonary aspergilloses [IPA] caused by *Aspergillus fumigatus*).

(C) Localization and diagnosis of single cancer cells and tumors (some peptides can interact specifically with important biomarkers of cancer cells and/or tumors (e.g., interaction of the labeled peptide GE-137 with the protein tyrosine kinase c-Met, overexpressed in colorectal cancer).

(D) Bioimaging.

maximum emission wavelength can be observed. These phenomena occur because the cell membrane environment is more viscous and less polar than water. Thus, the probe becomes more rigid (i.e., less vibrational modes), leading to a reduction in the thermal deactivation of excited states and increasing the amount of energy associated with radiative decay.

Non-fluorescent amino acids can became fluorescent by structural modifications, allowing their use as probes that minimally disturb peptide structure and function.[4,8,9] Non-natural FlAAs have been developed for insertion at specific positions of the peptide sequence without altering its biological function, both using solid-phase peptide synthesis and through genetic encoding.[4] For example, cyanotryptophans have been synthesized to improve the fluorescent properties of Trp by the insertion of cyanide (CN^-), an electron-withdrawing substituent.[10–12] Specifically, 5-cyanotryptophan showed an increased Stokes shift and enhanced sensitivity to hydration compared to Trp (Table 1; Figure 2A).[13] 5-Cyanotryptophan presents a Φ_{FL} of 0.01 and a predominant $t_{1/2}$ of 0.4 ns in water (Table 1). However, in other solvents, such as ethanol (Φ_{FL} = 0.17 and $t_{1/2}$ = 6.8), acetonitrile (Φ_{FL} = 0.13 and $t_{1/2}$ = 3.1), and 1,4-dioxane (Φ_{FL} = 0.11 and $t_{1/2}$ = 6.0), 5-cyanotryptophan displays greater Φ_{FL} and predominant $t_{1/2}$ compared to aqueous solution.[13] When mastoparan-X, an AMP from the mastoparan family that includes dozens of small cationic α-helical peptides, is labeled with 5-cyanotryptophan, it adopts a relatively unstructured conformation in water but remains folded into an α-helix similar to that of unlabeled mastoparan-X in the presence of dodecylphosphocholine micelles.[13] The 5-cyanotryptophan-labeled mastoparan-X exhibits a maximum fluorescence emission wavelength at 391 nm in water, with low fluorescence emission intensity.[13] However, in the presence of dodecylphosphocholine micelles, this labeled peptide presents an increased fluorescence emission intensity with a hypsochromic shift (from 391 to 372 nm).[13] These changes in the fluorescence profile of 5-cyanotryptophan-labeled mastoparan-X allow monitoring of its biological binding process.[13] Another example is L-4-cyanotryptophan (Figure 2A), a Trp derivative that has been used to label the AMP pHLIP within its N-terminal extremity.[14] This derivative exhibits higher Φ_{FL} in aqueous solution, a larger fluorescence $t_{1/2}$ and Stokes shift, and increased photostability compared to Trp (Table 1).[11,14] Due to its fluorescent

Table 1. Properties of Light-Emitting Probes

Probe	Exact Mass (g mol^{-1})	$\lambda_{abs.}$ (nm)	$\lambda_{em.}$(nm)	$\Delta\lambda$ (cm^{-1})	E (M^{-1} cm^{-1})	Φ_{FL}	$t_{1/2}$ (ns)	Ref.
Natural fluorescent amino acids								
Trp	204.09	280	348	6,980	5,600	0.20	3.1 and 0.5	Ghisaidoobe and Chung[6]
Tyrosine	181.07	274	303	3,500	274	0.14	3.6	Ghisaidoobe and Chung[6]
Phenylalanine	165.08	257	282	3,450	200	0.04	6.4	Ghisaidoobe and Chung[6]
Non-natural fluorescent amino acids								
L-4-Cyanotryptophan	229.09	312	420	8,240	6,000	0.80	13.7	Hilaire et al.[11]
5-Cyanotryptophan	229.09	280	391	10,140	5,500	0.01	0.4	Markiewicz et al.[13]
Trp(BODIPY)	526.24	503	517	540	121,000	0.22[c]	–	Mendive-Tapia et al.[15]
Trp(redBODIPY)	594.21	570	590	600	52,950	–	–	Subiros-Funosas et al.[17]
Acd	282.10	400	450	2,780	5,700	0.95	15.0	Sungwienwong et al.[21]
Mcm	263.08	320	390	5,610	–	–	–	Sungwienwong et al.[21]
Aad	297.11	425	530	4,660	–	–	–	Sungwienwong et al.[21]
Fluorescent organic probes								
GFP	27,000	395/475	508	5,630/1.370	56,000	0.60	–	Johnson and Straight[23]
Rhodamine B	478.20	554	576	690	106,000[a]	0.65[b]	1.5–1.7	Kubin and Fletcher[27] and Kristoffersen et al.[28]
Fluorescein (dianion)	330.05	490	515	990	76,900	0.93	4.1	Sjöback et al.[29]
Coumarin 343	285.10	443	462	930	44,300[b]	0.63[b]	4.6	Pant and Girault[34]
DMAQs	282.09–410.25[a]	274–498	469–550	–	–	–	–	Jun et al.[35]
CPX	488.21	419	542	5,420	–	–	–	Jun et al.[36]
HC	411.22	670	718	1,000	100,225	0.43[b]	–	Jin et al.[44]
Cy5**	887.22	648	675	620	–	–	–	Burggraaf et al.[50]
Cy5.5	583.33	680	708	580	–	–	–	Joshi et al.[51]

Values corresponding to the exact mass, maximum absorbance wavelength ($\lambda_{abs.}$), maximum emission wavelength ($\lambda_{em.}$), Stokes shift ($\Delta\lambda$), molar absorptivity (ε), fluorescence quantum yield (Φ_{FL}), and lifetime ($t_{1/2}$) are provided for natural fluorescent amino acids, non-natural fluorescent amino acids, and fluorescent organic probes. All of the fluorescence properties presented in this table were established in aqueous solution, except when specified: [a](methanol), [b](ethanol), and [c](membrane environment).

properties, L-4-cyanotryptophan has been used as a donor fluorescence resonance energy transfer (FRET) pair with 3,3¢-dioctadecyloxacarbocyanine perchlorate to determine the rate constant for peptide-membrane binding.[14]

Another Trp-derived synthetic amino acid, Trp(BODIPY), was designed by conjugating Trp and boron-dipyrromethene (BODIPY) fluorogen via a spacer-free C-C bond (Figure 2A; Table 1).[15] Trp(BODIPY) has been used to label short peptides such as PAF26, an antimicrobial hexapeptide with high affinity toward the *Aspergillus fumigatus* cell membrane.[15] This fungus is responsible for invasive pulmonary aspergilloses (IPA), with a mortality rate of up to 40%.[16] The high stability of this probe allowed *ex vivo* imaging of human pulmonary tissue during an IPA infection with minimal fluorescence background from the tissue (Figure 1B).[15] Red-emitting fluorescent probes have attracted attention due to their less-energetic emission, which causes less damage to biological samples. Recently, the first red-emitting Trp-based fluorescent amino acid, also containing BODIPY in its structure (Trp(redBODIPY); Figure 2A; Table 1), was synthesized and coupled to the hydrophobic portion of a cyclic peptide to label the protein keratin 1, a diagnostic marker for breast cancer (Figure 1C).[17] Computational and experimental results showed that the unlabeled peptide and the same peptide labeled with Trp(redBODIPY) presented similar values of relative binding affinity with keratin 1 (k_d ~1.0 μmol L^{-1}).[17]

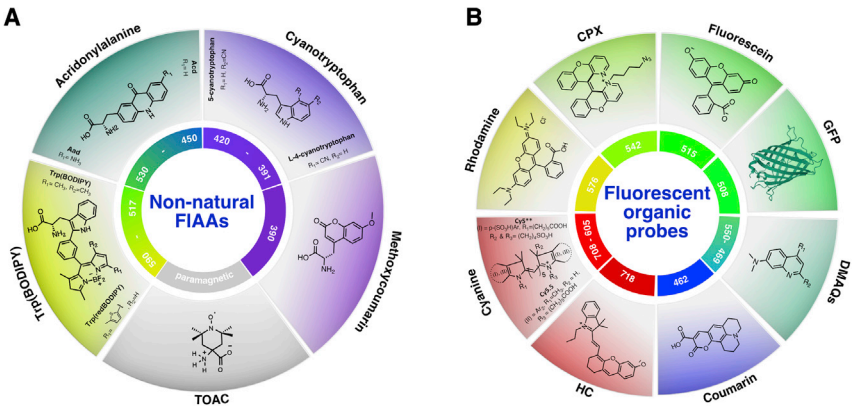

Figure 2. Fluorescent Probes for Peptide Labeling

Schematic representation of the relationship between molecular structure (depending on the identity of the substituents), the color of the light emitted through the fluorescence decay, and the maximum emission wavelength ($\lambda_{em.}$) of (A) non-natural fluorescent amino acids and (B) fluorescent organic probes.

Nonetheless, the same peptide labeled with the commercial red fluorescent probe BODIPY TR (at the amino group within the side chain of D-Lys) presented a 5-fold weaker binding profile.[17] Therefore, Trp(redBODIPY) interfered less with the peptide-keratin 1 affinity process than BODIPY TR.[17]

The first spin label probe incorporated through a peptide bond was TOAC (2,2,6,6-tetramethyl-*N*-oxyl-4-amino-4-carboxylic acid), a non-natural amino acid containing a stable paramagnetic nitroxide radical (Figure 2A).[18] Recently, TOAC was used to label tritrpticin (TRP3), an AMP that acts by a toroidal pore mechanism and has at least four different conformations in solution, with a turn-turn structure in its C-terminal portion stabilized in the presence of micelles, which can be observed by NMR.[19] TRP3 was labeled with TOAC at its N-terminal extremity (TOAC^0-TRP3), and internally, by substituting the proline residue in position five (TOAC5-TRP3) to elucidate its mechanism of action (Figure 1A), activity, toxicity, and conformational properties.[20] Both TOAC-labeled peptides presented similar activity against *Escherichia coli* (minimum inhibitory concentration [MIC] = 4.0, 1.3 and 1.9 μmol L^{-1} for TOAC^0-TRP3, TOAC5-TRP3, and TRP3, respectively), and *Micrococcus luteus* (MIC ~4.0 and 1.1 μmol L^{-1} for TOAC-labeled peptides and TRP3, respectively) compared to non-labeled TRP3.[20] All of the peptides showed low hemolytic activity (<5%) at concentrations 25-fold higher than their MIC. In addition, compared to its template TRP3, the labeled N-terminal extremity led to a similar complex structure, but was more effective at membrane permeabilization. On the contrary, when TRP3 was labeled in the middle of its sequence, it exhibited similar mechanisms of action as when unlabeled but with an extended conformation.[20]

Acridonylalanine (Acd, Figure 2A) is another widely used non-natural FlAA. Acd can be used for labeling and as a pair for FRET or photoinduced electron transfer.[21] It displays a high Φ_{FL} in water, long fluorescence $t_{1/2}$, and high photostability, compared to other non-natural FlAAs (Table 1).[21] Acd and the small probe methoxycoumarinylalanine (Mcm; Figure 2A; Table 1) were used as a FRET pair to study protein distances at a range of 15–40 Å. Trp labeling with the FRET pair Mcm/Acd has been used to monitor multiple interactions simultaneously (e.g., protein/protein interactions and conformational changes) in three-color FRET.[22] However, Acd has a small Stokes shift and its emission spectra shows a significant overlap with that of

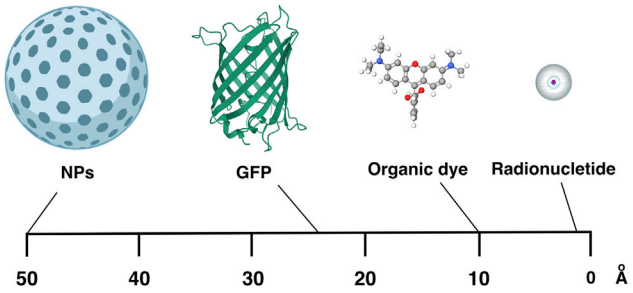

Figure 3. Size Distribution of Light-Emitting Probes Used for Peptide Labeling
Comparison between the structure and size of different types of fluorescent probes that are currently applied for labeling peptides.

Mcm (Table 1). To further improve the Mcm/Acd FRET, an Acd derivative (aminoacridonylalanine, Aad) was synthesized and presented a bathochromic shift at its maximum emission wavelength with the insertion of an amino group as substituent (Figure 2A; Table 1).[21] Aad was shown to be a better FRET acceptor than Acd when used with the Mcm donor. Furthermore, its increased Stokes shift allowed the use of Aad as a FRET donor for red wavelength dyes and microscopy applications using conventional filter sets for cyan fluorescent protein excitation and yellow fluorescent protein emission.[21]

Fluorescent Organic Probes

Green fluorescent protein (GFP, Figure 2B; Table 1), isolated from the jellyfish *Aequorea victoria*, is the most common fluorophore in molecular biology and biotechnology, and is widely used as a marker for gene expression and protein localization in living and fixed tissues.[23] Other self-labeling fluorescent proteins (FPs), such as SNAP-tag and HaloTag, can be conjugated to peptides or proteins to investigate how they associate with cell membranes, or can even be directly coupled to living cells.[23,24] However, wild-type FPs are usually found in their oligomeric form, showing higher toxicity and decreased ability to interact with their target biomolecules (e.g., proteins, peptides), leading to mistargeting and lower selective binding, thus requiring artificial monomerization, and consequent loss of brightness and stability.[23] Moreover, FPs are large and hydrophobic (Figure 3), and when they are incorporated into small target molecules such as peptides, they can cause undesirable aggregation and changes in physicochemical properties and biological activity.[25,26] Fluorescent organic probes, such as xanthene dyes (e.g., rhodamine B, fluorescein; Figure 2B), represent an alternative for peptide labeling as they are smaller in size (Figure 3) and exhibit greater water solubility and Φ_{FL} (Table 1).[27–29] Nonetheless, such organic probes may also compromise the activity of peptides, which are sensitive to alterations in structure and physicochemical properties. Hydrophobicity and net charge are the most relevant features affected in these cases and can yield peptides with high toxicity (Figure 3). For instance, an oligopeptide (EVP50) labeled with rhodamine B (Figure 2B; Table 1) showed lethal toxicity toward zebrafish larvae (lethal dose 50% [LD_{50}] = 6 μmol L^{-1}) accumulating inside the cells within minutes, and interfering with calcium homeostasis and membrane dysfunction, whereas the unlabeled EVP50 did not display cytotoxicity *in vitro* or *in vivo*.[30] Crotamine is a cell-penetrating peptide (CPP) with antitumor, antimicrobial, antifungal, and antiparasitic activities at micromolar concentrations, which also exhibits toxicity against eukaryotic muscle cells and tissues at millimolar concentrations.[31] The rhodamine B-labeled crotamine was toxic at micromolar concentrations (4.0 μmol L^{-1}), translocating the vitelline membrane, and accumulating in the zebrafish yolk sac,

leading to zebrafish larvae death in <10 min. Moreover, at lower concentrations (< 1.0 μmol L^{-1}), the labeled crotamine caused malformation in embryos, delayed or completely halted hatching, decreased cardiac functions, and attenuated swimming distance of zebrafish.[32] Xanthene dyes can also be used to study the MoA of AMPs (Figure 1A); however, their hydrophobicity may decrease their antimicrobial activity and alter the MoA of these peptides.[33] The enteric peptide α-defensin HD5 presents antimicrobial activity by generating bleb conformations and elongation of the treated bacteria, suggesting a different MoA from classical membrane-disrupting peptides.[33] To study its MoA against bacterial cells (Figure 1A), α-HD5 was labeled with rhodamine B, coumarin 343, and fluorescein at different positions within its sequence (Figure 2B; Table 1).[33,34] Rhodamine B-labeled α-HD5 enabled tracking of the peptide to the poles and cytoplasm division site of the bacterial cell, indicating that α-HD5 operates internally within the cell and targets cell division. However, labeling with rhodamine B repressed the antibacterial activity of this peptide when compared with its unlabeled counterpart.[33]

Despite the discovery of a number of fluorescent probes for peptides, several issues still need to be addressed to yield probes with high sensitivity and Φ_{FL} that lack toxicity, can be easily coupled to the peptide backbone, and do not alter structure, physicochemical properties, or biological activity. Overcoming these issues is still a challenge, but progress has been made. Recently, small and adaptable quinoline-based probes containing three functionalizable domains were synthesized by a simple and efficient methodology.[35] More than 20 derivatives were designed from a "core" scaffold of dimethylamino quinoline (DMAQ; Figure 2B; Table 1). The derivatives exhibited unusual pH sensitivity in multicolor live-cell imaging.[35] Also, a water-soluble, cell-permeable, and non-cytotoxic photoconvertible small fluorescent probe called CPX was synthesized (Figure 2B; Table 1).[36] CPX was coupled at three different positions within the α-synuclein protein through Huisgen 1,3-dipolar azide-alkyne cycloaddition and, due to its small size, overcame the common limitations of FPs in studies involving α-synuclein aggregate dynamics (Figure 3).[36] Moreover, the precursor of this probe can be conjugated to other biomolecules through nucleophilic displacement of the iodide.[36]

Proteolytic degradation is a major obstacle in the development of new peptide-based drugs. Fluorescent quenchers, such as thioamides, can be used to track and reduce proteolytic degradation, thus stabilizing and increasing the *in vivo* serum half-life of peptides.[37,38] Cysteine protease can be tracked through the synthesis of thioamide-labeled peptides.[39] When the peptide is cleaved, the thioamide group stops quenching and fluorescence can be observed. The proteolytic degradation of 5 papain families was reduced when thioamide was placed near or exactly at the scissile bond of the peptide backbone, making the peptide 750-fold more stable.[39]

Fluorescent probes are limited *in vivo* (Figure 1D), particularly when applied in humans, due to the matrix interference by autofluorescence and limited tissue penetration (1–2 mm) when their maximum emission wavelength is <650 nm.[40] To overcome these hurdles, nonlinear optical microscopy techniques, such as two-photon microscopy, have been used for high-resolution imaging in tissues, enabling better tissue penetration using two-photon probes.[41] However, non-toxic probes with effective two-photon properties that absorb long-wavelength excitation light and are used at low concentrations without causing tissue damage are still needed. Thus, novel noninvasive near-infrared (NIR) fluorescent probes, which emit in the NIR region, 650–900 nm, are urgently needed for monitoring enzymatic activities and for cancer

diagnostics. Contrary to short-wavelength fluorescent dyes, these probes have low autofluorescence and light scattering, generate minimal photodamage to biological samples, and undergo deep-tissue penetration (1–10 cm).[42] The NIR probe HC (Figure 2B; Table 1) has been successfully applied for the detection of β-glucuronidase (GLU) activity, an important biomarker for cancerous cells and the intestinal metabolism of drugs (Figure 1C).[43,44] HC can be used to visualize GLU in a tumor-bearing mouse model and in the intestinal tract of living mice and zebrafish with high selectivity and sensitivity, desirable cell penetration, and low cytotoxicity.[44]

NIR cyanine probes are used for detecting mRNA,[45] H_2S,[46] nucleic acid,[47] and mitochondrial cysteine,[48] as well as for labeling DNA,[49] enzymes, and peptides that specifically target overexpressed proteins in cancer, such as tyrosine kinase c-Met (Figure 1C).[50] The NIR cyanine probe (Cy5**; Figure 2B; Table 1) has been used for labeling a 26-amino-acid-residue-long cyclic peptide that targets the human tyrosine kinase c-Met, a biomarker for early-stage colorectal cancer (Figure 1C).[50] The labeled peptide, GE-137, was tested *in vitro*, *in vivo* (Figure 1D), and in a pilot study with human patients by intravenous administration. GE-137 was safe in humans and enabled the visualization of 36 hyperplastic lesions and 8 serrated polyps by colonoscopy.[50] Another cyanine probe (Cy5.5; Figure 2B; Table 1) was used for labeling a peptide (KSP*) whose amino acid sequence was modified using structural modeling based on mimotopes to optimize its hydrophilic and hydrophobic interactions with HER2, a receptor that is overexpressed in tumoral colorectal cells of sessile serrate and sporadic adenoma in the proximal colon (Figure 1C).[51] The labeled peptide helped localize spontaneous adenomas and enabled real-time *in vivo* imaging (Figure 1D) with high binding affinity, low signal-to-noise ratio, and deeper tissue penetration when compared to the same peptide labeled with fluorescein isothiocyanate.[51]

Radionuclides

Radionuclides that emit a positron when they undergo radioactive decay such as ^{68}Ga, 18Fl, 13N, and 15O can be used for labeling peptides in positron emission tomography/computed tomography (PET/CT) studies.[52] The main advantage of radionuclides over FPs and fluorescent organic probes for peptide labeling is their reduced size (Figure 3). The AMP ubiquicidin (UBI), for example, displays low toxicity toward mammalian cells, binds specifically to the bacterial cell membrane, and is widely used in nuclear imaging for infection detection when labeled with ^{68}Ga.[53–56] UBI has been functionalized with a chelator (1,4,7-triazacyclononane-1,4,7-triacetic acid [NOTA]) and complexed with ^{68}Ga to study its cytotoxicity *in vitro*, in addition to its biodistribution, pharmacokinetics, and radiation dosimetry in non-human primates. These results led to the first-in-human evaluation of infection diagnosis using PET/CT imaging.[57,58] Ga-NOTA-UBI lacked toxicity, displayed favorable biodistribution (with predominant urinary excretion), and safety for human applications, as it was able to detect bone and soft-tissue infection with no side effects observed.[57]

Presently, some radionuclides, including ^{111}In, ^{90}Y, and ^{177}Lu, have been used in peptide receptor radionuclide therapy (PRRT) as a strategy for the treatment and diagnosis of neuroendocrine tumors, metastatic pheochromocytoma, and paraganglioma (PPGL).[59] PRRT involves the use of radiolabeled somatostatin analogs that bind to somatostatin receptors, which are overexpressed by neuroendocrine tumors and PPGL (Figure 1C).[59] This radiotherapy allows the delivery of radionuclides to tumor cells, dosimetry studies, and localization of tumors. The most used somatostatin analog peptide is octreotide labeled with ^{177}Lu (^{177}Lu-DOTATATE)

or ^{90}Y (^{90}Y-DOTATOC), in which ^{90}Y presents higher toxicity in relation to ^{177}Lu.[60,61] An analysis from the NETTER-1 trial, an international phase III study in patients with midgut neuroendocrine tumors, demonstrated that treatment with ^{177}Lu-DOTA-TATE significantly improved progression-free survival and global health status in patients with progressive midgut neuroendocrine tumors compared with a high-dose of octreotide. Treatment reduced insomnia, fatigue, pain, loss of appetite, and diarrhea.[62] Nonetheless, the radiation generated during PRRT therapy may produce severe side effects.[59]

Malignant prostate epithelial cells overexpress gastrin-releasing peptide receptor (GRPr) and prostate-specific membrane antigen (PSMA) at levels up to 1,000-fold higher than normal prostate cells.[63] Small peptides that bind selectively to PSMA can be used as an alternative therapy to deliver cytotoxic drugs to malignant sites (Figure 1C).[63–66] These peptides have been labeled with radionuclides using chelators such as DOTA, NODAGA, or HBED-CC. The peptide bombesin (BN), for example, binds selectively to GRPr, an observation that led to the development of a number of BN-based radiopharmaceuticals for prostate cancer diagnosis.[67,68] A ^{177}Lu-labeled BN peptide (^{177}Lu-iPSMA-BN) was synthesized, and its ability to target PSMA and GRPr was evaluated *in vitro* and *in vivo*. The resulting molecule was considered a stable and specific radiopharmaceutical for prostate cancer.[68] However, the pharmacokinetics of these therapeutic agents should be further investigated, especially because radiotracers may accumulate in the pancreas leading to side effects, particularly when administering high doses of radiolabeled peptides.[58]

Nanoparticles

Nanoparticles (NPs; Figure 3) have been designed for tracking therapeutic biomolecules, drug delivery, improvement of the solubility and half-life of certain drugs, and for reducing immunogenicity.[69] Peptide-based NPs with structure-induced fluorescence represent a new strategy for biological imaging that allows imaging cells and tissues without the need for fluorescent probes. Such NPs have been described as functional nanoprobes because of their biological activity and fluorescent properties.[70] NIR fluorescent cyclic peptide NPs (f-PNPs) were designed and synthesized for imaging and drug delivery applications in esophageal cancer.[71] f-PNPs were conjugated with RGD (i.e., Arg-Gly-Asp) moieties for the selective targeting of esophageal cancer cells via integrin receptors, and embedded with epirubicin (EPI), a chemotherapeutic drug that can cause side effects such as cardiac toxicity, bone marrow suppression, and secondary leukemia.[71] The resulting complex was used to monitor EPI delivery in tumors by NIR fluorescence (NIRF), demonstrating a significant reduction in cardiotoxicity and enhanced antitumor activity in relation to EPI alone.[71] Another interesting alternative is the use of polymers that can emit strong fluorescence by aggregation-induced emission (AIE).[72] Novel nanoengineered peptide-grafted hyperbranched polymers (NPGHPs) were synthesized by ring-opening polymerization on the surface of the hyperbranched polyamide amine (H-PAMAM), a polymer containing tertiary amines that, when oxidized, becomes fluorescent via AIE.[73,74] NPGHPs were used as fluorescent probes to visualize antibacterial activity, allowed monitoring of *E. coli* with a limit of detection of 10^4 colony-forming units (CFU) mL^{-1}, and showed potent antimicrobial activity against *E. coli*, *Pseudomonas aeruginosa*, *Staphylococcus aureus*, and *Bacillus subtilis*. The hemolytic activity of NPGHPs was examined using fresh anticoagulant rabbit blood, presenting 2.13% hemolysis rate when using 200 μg mL^{-1} of NPGHPs. Also, toxicity was verified using mouse embryonic osteoblast precursor cells, showing >80% cell survival rate at a concentration ranging from 25 to 200 μg mL^{-1} after 3 days.[73]

Quantum dots (QDs) are NPs of 1–10 nm in diameter (Figure 3) that contain a metallic core usually based on zinc or cadmium. QDs can display antimicrobial activity and inhibit biofilm formation.[75] QDs represent a promising alternative for the labeling of peptides, proteins, oligonucleotides, and polysaccharides in addition to being used for imaging single cells, tissue, and tumors.[76] QDs have advantages over organic probes due to their satisfactory Stokes shifts, which increases as their diameter decreases, $t_{1/2}$ of 10–40 ns, high Φ_{FL}, large extinction coefficients (10- to 50-fold higher than organic probes), and broad excitation and emission spectra.[42,77–79] Two AMPs, KG18 and VR18, were conjugated with tungsten disulfide (WS_2) QDs for applications in antimicrobial therapy, diagnosis, and bioimaging (Figure 1D).[80] The resulting conjugations demonstrated antibiofilm potency (at 200 μmol L^{-1}) and 2-fold higher antimicrobial activity (2.5 μmol L^{-1}) than non-conjugated peptides against *P. aeruginosa* and *Candida albicans*, causing membrane rupture, loss of morphology, and metabolite release within a few minutes of treatment. The larger surface area of the conjugated peptide QDs, compared to the peptide alone, caused peptide clustering and consequently more efficient membrane disruption. Furthermore, the use of QDs enabled monitoring the precise location of QD-KG18 within *C. albicans* cells as early as 10 min after incubation, whereas both AMPs (i.e., KG18 and VR18) labeled with fluorescein isothiocyanate remained at the cell surface even after 60 min of incubation.[80] Nevertheless, QDs have limitations when continuously exposed to light, generating a "blinking effect" and toxicity, likely due to the release of metal ions or reactive oxygen species. Moreover, QDs can translocate cellular membranes and interact with functional biomolecules migrating to various organs and tissues, ultimately causing damage.[42,76] Different strategies have been designed in an attempt to overcome these limitations, such as coating QDs with polyethylene glycol, dihydrolipoic acid, and peptides, to increase stability and protect the core from degradation.[76] The AMP indolicidin was used to coat and protect the metallic core of toxic antimicrobial QDs, reducing their toxicity.[81] The antimicrobial activity of these indolicidin-coated QDs against *S. aureus*, *P. aeruginosa*, *E. coli* and *Klebsiella pneumoniae* was compared with that of QDs and indolicidin alone.[81] In addition, ecotoxicological tests were performed for QDs and indolicidin-coated QDs to evaluate the immobilization of *Daphnia magna*, the bioluminescence (BL) inhibition of *Vibrio fisheri*, the mutagenicity activity of *Salmonella typhimurium* TA 100, the genotoxicity on *Daphnia magna*, as well as analysis of reactive oxygen species and antioxidant enzyme activity on *Daphnia magna*.[81] The indolicidin-coated QDs showed enhanced antimicrobial activity compared to QDs and indolicidin, mainly against Gram-negative bacteria. QDs coated with indolicidin exhibited decreased ecotoxicity against *Daphnia magna*, compared to QDs (from 67% of mortality for QDs to 20% for coated QDs), bioluminescence inhibition in *Vibrio fisheri* (~40% with 5.0 nmol L^{-1}), and no mutations in *S. typhimurium* TA 100. However, both QDs alone and indolicidin-coated QDs induced deleterious effects such as oxidative stress and DNA damage.[81]

Chemiluminescence (CL) and BL Imaging

CL is the generation of light resulting from an exothermic chemical reaction.[82] When this phenomenon occurs inside a living organism, it is called BL.[82] Many CL and BL transformations have been thoroughly studied at the molecular level, both experimentally and using theoretical data.[82] Light is produced when the electronic excited state of a molecule decays through the emission of a photon. Such emissive excited states can be obtained by a chemical transformation, usually involving a multistep complex sequence of reactions.[82] Associated with peptides, CL and BL systems have been extensively used for analytical purposes, as discussed recently elsewhere.[83] Here, we focus on how CL and BL can be applied

to assess dynamic aspects (e.g., real-time kinetics, chemical environment) related to peptides.

To produce the electronic excited state, one can rely on an electrochemical process coupled to chemical transformation known as electrochemiluminescence (ECL). ECL has been used to detect and quantify peptides and other target molecules.[83,84] Moreover, information regarding dynamic aspects, such as intracellular uptake and the enzymatic activity of associated enzymes that are associated with peptides, can be obtained using CL systems that involve cyclic peroxides as substrates or reaction intermediates. The most commonly used cyclic peroxides are phenoxy-substituted adamantylidene-1,2-dioxetanes,[85–87] also known as Schaap's 1,2-dioxetanes (S12D; Figure 4).[88] The phenoxy portion of the 1,2-dioxetane contains a protecting group (also known as a trigger) that can be removed upon the addition of an external reactant, triggering peroxide decomposition and the generation of carbonyl fragments on the excited state, ultimately leading to CL emission.[82,85]

Modern approaches have used a self-immolative scaffold to enable the release of a molecule of interest *in situ*, together with the generation of the CL signal. This has been done with a self-immolative CL prodrug, containing S12D as a CL probe and a peptide-derived chemotherapeutic agent (monomethyl auristatin E [MMAE]) with disassembling being triggered by β-galactosidase.[86,87] Green 550 nm CL light intensity increased with higher concentrations of MMAE, allowing for real-time monitoring of endogenous enzymatic activity in mouse tumors overexpressing β-galactosidase.[87] Caspase-3 activity has been measured by using S12D as a CL probe, and *para*-aminobenzylic alcohol (PABA) as a self-immolative spacer attached to an Asp-Glu-Val-Asp peptide responsive to the enzyme.[89]

Luminol is a well-known CL reagent.[82] Although luminol itself is not a cyclic peroxide, a six-membered peroxidic system is produced as an intermediate after reaction with H_2O_2 in basic media and in the presence of metallic ions as catalysts.[82] The decomposition of such six-membered peroxidic intermediate generates excited states and, consequently, fluorescence emission.[82] Some luminol derivatives have been applied as CL probes for peptides instead of S12D.[90,91] The Asp-Glu-Val-Asp tetrapeptide was used as a linker of a luminol derivative (*N*-(4-aminobutyl)-*N*-ethylisoluminol [ABEI]) coupled to functionalized magnetic beads (MBs; Figure 4).[90] Upon peptide cleavage by caspase-3, the released ABEI was recovered and its CL reaction with H_2O_2 and Co^{2+} was used for enzyme activity determination.[90] The use of luminol derivatives as CL probes does not allow for real-time measuring, in contrast to S12D derivatives when they are used as sources for light production. Nonetheless, saturation kinetics for the enzymatic activity of caspase-1 was observed with the flow-injection method, using ABEI molecules as a CL substrate coupled to gold nanoparticles. The latter were recuperated from their conjugates with MBs and Tyr-Val-Ala-Asp, previously treated with caspase-1.[91]

Recently, a chemo-fluoro-luminescent reporter (CFR) has been used in what the authors referred to as "duplex imaging" of drug-induced hepatotoxicity (DIH),[85,92] although in this case CL was not involved in peptide cleavage. The CFR comprised a S12D molecule (with the phenoxy group protected by a triflate group [Tf]) connected to a hemicyanine unit (CyU) with its hydroxyl group caged by a PABA linker, in turn conjugated to a caspase-3-cleavable Asp-Glu-Val-Asp peptide.[92] Caspase-3 induced cleavage of the amide bond between the tetrapeptide and the self-immolative PABA linker, producing CyU after a 1,6-elimination; due to its structure, CyU exhibited strong NIRF. In turn, S12D CL was triggered by Tf deprotection with superoxide anion,

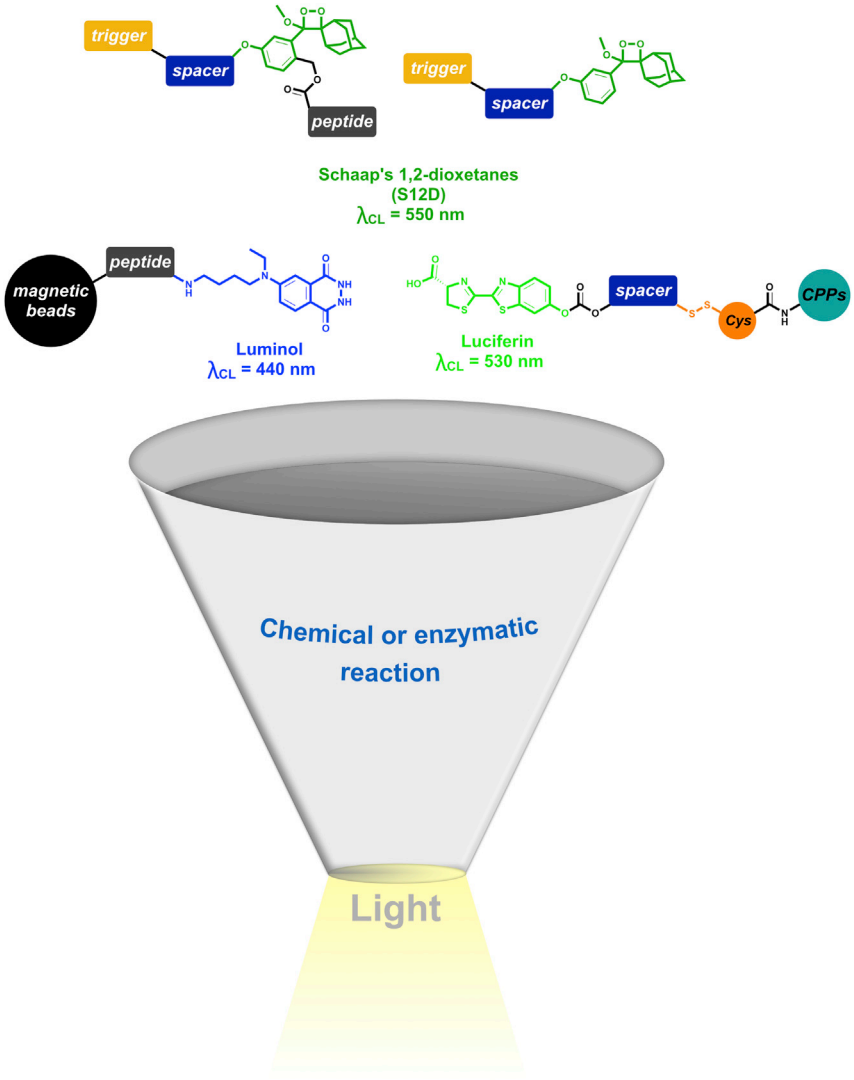

Figure 4. Molecular Structures of Chemiluminescent and Bioluminescent Probes, Assembled with Generic Peptides, Spacers, and Triggers (Structures Not Shown)

Chemical-induced decomposition of S12D and luminol, as well as the luciferin enzymatic reaction with luciferase, generates the corresponding decomposition products and light at the given wavelengths.

since superoxide anion attacks the sulfonate ester group.[93] According to the authors, CFR enables the longitudinal measurement of oxidative stress and cellular apoptosis in a two-channel imaging method, hence the term "duplex imaging."[92]

Real-time imaging has been successfully performed using BL probes based on the firefly luciferin/luciferase pair.[94] Contrary to triggered-CL of peroxides such as S12D, light emission in BL depends on the interaction of the luciferin substrate (Figure 4) with the enzyme luciferase in the presence of molecular oxygen and cofactors such as ATP.[82] A 1,2-dioxetanone high-energy intermediate is generated following a complex set of reactions, and the decomposition of this cyclic peroxide furnishes oxyluciferin in the electronic excited state.[82] Deactivation of oxyluciferin generates light at 530 nm that can be conveniently used for the quantification of cell transporters.[94]

Luciferin has also been used as a BL reporter for the real-time imaging of CPP intracellular uptake (Figure 4). Firefly luciferin has been linked to an octa-arginine transporter using a dithiol group, enabling the readout of real-time BL kinetics in a prostate cancer cell line stably transfected with luciferase (PC3M-luc).[94] Using HeLa pLuc 705 cells, the uptake intracellular kinetics of eight well-known CPPs linked to luciferin were addressed and compared.[95] Peptides MAP and TP10 displayed fast internalization rates, resembling membrane-permeable free luciferin, whereas the slow uptake of *p*Vec, penetratin, M918, and EB1 were shown to be consistent with endocytosis mechanism of internalization.[95] Following the general concept of CPPs linked to luciferin, firefly luciferase-specific inhibitors (FLICs)[96] and split luciferin peptide (SLP)[97] methodologies have been proposed, the latter being suitable for real-time imaging both *in vitro* and *in vivo*.

Concluding Remarks

Despite recent progress made in this research area, the development of suitable light-emitting probes for labeling small molecules such as peptides remains a grand challenge. The lack of non-toxic light emitting probes for labeling peptides, while not negatively affecting their specificity and biological and structural properties, has hindered progress in this field. Here, we provide a summary of the latest efforts aimed at developing small and appropriate fluorescent and luminescent probes. While there is more work to be done to develop minimalistic structural modifications yielding luminescence and thus enabling imaging, we anticipate that such advances would accelerate the broad use of fluorescent approaches for disease diagnosis and detection.

ACKNOWLEDGMENTS

C.F.-N. holds a Presidential Professorship at the University of Pennsylvania, is a recipient of the Langer Prize by the AIChE Foundation, and acknowledges funding from the National Institute of General Medical Sciences of the National Institutes of Health under award no. R35GM138201, the Institute for Diabetes, Obesity, and Metabolism, and the Penn Mental Health AIDS Research Center of the University of Pennsylvania. We thank the Fundação de Amparo à Pesquisa do Estado de São Paulo (FAPESP) for the provided grants (A.B., 2016/10585-4 and 2019/15871-3) and Xunta de Galicia for a pre-doctoral fellowship 2019 co-funded with the European Social Fund (FSE) of the European Union (ED481A-2019/081).

REFERENCES

1. de la Fuente-Nunez, C., Torres, M.D., Mojica, F.J., and Lu, T.K. (2017). Next-generation precision antimicrobials: towards personalized treatment of infectious diseases. Curr. Opin. Microbiol. *37*, 95–102.

2. Marqus, S., Pirogova, E., and Piva, T.J. (2017). Evaluation of the use of therapeutic peptides for cancer treatment. J. Biomed. Sci. *24*, 21.

3. Kumar, P., Kizhakkedathu, J.N., and Straus, S.K. (2018). Antimicrobial Peptides: Diversity, Mechanism of Action and Strategies to Improve the Activity and Biocompatibility In Vivo. Biomolecules *8*, 4.

4. Cheng, Z., Kuru, E., Sachdeva, A., and Vendrell, M. (2020). Fluorescent Amino Acids as Versatile Building Blocks for Chemical Biology. Nat. Rev. Chem. *4*, 275–290.

5. Vivian, J.T., and Callis, P.R. (2001). Mechanisms of tryptophan fluorescence shifts in proteins. Biophys. J. *80*, 2093–2109.

6. Ghisaidoobe, A.B.T., and Chung, S.J. (2014). Intrinsic tryptophan fluorescence in the detection and analysis of proteins: a focus on Förster resonance energy transfer techniques. Int. J. Mol. Sci. *15*, 22518–22538.

7. Würth, C., Grabolle, M., Pauli, J., Spieles, M., and Resch-Genger, U. (2013). Relative and absolute determination of fluorescence quantum yields of transparent samples. Nat. Protoc. *8*, 1535–1550.

8. Navo, C.D., Asín, A., Gómez-Orte, E., Gutiérrez-Jiménez, M.I., Compañón, I., Ezcurra, B., Avenoza, A., Busto, J.H., Corzana, F., Zurbano, M.M., et al. (2018). Cell-Penetrating Peptides Containing Fluorescent d-Cysteines. Chemistry *24*, 7991–8000.

9. Wörner, S., Rönicke, F., Ulrich, A.S., and Wagenknecht, H.A. (2020). 4-Aminophthalimide Amino Acids as Small and Environment-Sensitive Fluorescent Probes for Transmembrane Peptides. ChemBioChem *21*, 618–622.

10. Talukder, P., Chen, S., Roy, B., Yakovchuk, P., Spiering, M.M., Alam, M.P., Madathil, M.M., Bhattacharya, C., Benkovic, S.J., and Hecht, S.M. (2015). Cyanotryptophans as Novel Fluorescent Probes for Studying Protein Conformational Changes and DNA-Protein Interaction. Biochemistry *54*, 7457–7469.

11. Hilaire, M.R., Ahmed, I.A., Lin, C.W., Jo, H., DeGrado, W.F., and Gai, F. (2017). Blue fluorescent amino acid for biological spectroscopy and microscopy. Proc. Natl. Acad. Sci. USA *114*, 6005–6009.

12. Boville, C.E., Romney, D.K., Almhjell, P.J., Sieben, M., and Arnold, F.H. (2018). Improved Synthesis of 4-Cyanotryptophan and Other Tryptophan Analogues in Aqueous Solvent Using Variants of TrpB from Thermotoga maritima. J. Org. Chem. *83*, 7447–7452.

13. Markiewicz, B.N., Mukherjee, D., Troxler, T., and Gai, F. (2016). Utility of 5-Cyanotryptophan Fluorescence as a Sensitive Probe of Protein Hydration. J. Phys. Chem. B *120*, 936–944.

14. Zhang, K., Ahmed, I.A., Kratochvil, H.T., DeGrado, W.F., Gai, F., and Jo, H. (2019). Synthesis and application of the blue fluorescent amino acid l-4-cyanotryptophan to assess peptide-membrane interactions. Chem. Commun. (Camb.) *55*, 5095–5098.

15. Mendive-Tapia, L., Zhao, C., Akram, A.R., Preciado, S., Albericio, F., Lee, M., Serrels, A., Kielland, N., Read, N.D., Lavilla, R., and Vendrell, M. (2016). Spacer-free BODIPY fluorogens in antimicrobial peptides for direct imaging of fungal infection in human tissue. Nat. Commun. *7*, 10940.

16. Chai, L.Y.A., and Hsu, L.Y. (2011). Recent advances in invasive pulmonary aspergillosis. Curr. Opin. Pulm. Med. *17*, 160–166.

17. Subiros-Funosas, R., Ho, V.C.L., Barth, N.D., Mendive-Tapia, L., Pappalardo, M., Barril, X., Ma, R., Zhang, C.-B., Qian, B.-Z., Sintes, M., et al. (2020). Fluorogenic Trp(RedBODIPY) Cyclopeptide Targeting Keratin 1 for Imaging of Aggressive Carcinomas. Chem. Sci. (Camb.) *11*, 1368–1374.

18. Schreier, S., Bozelli, J.C., Jr., Marín, N., Vieira, R.F.F., and Nakaie, C.R. (2012). The spin label amino acid TOAC and its uses in studies of peptides: chemical, physicochemical, spectroscopic, and conformational aspects. Biophys. Rev. *4*, 45–66.

19. Schibli, D.J., Hwang, P.M., and Vogel, H.J. (1999). Structure of the antimicrobial peptide tritrpticin bound to micelles: a distinct membrane-bound peptide fold. Biochemistry *38*, 16749–16755.

20. Bozelli, J.C., Jr., Salay, L.C., Arcisio-Miranda, M., Procopio, J., Riciluca, K.C.T., Silva Junior, P.I., Nakaie, C.R., and Schreier, S. (2020). A comparison of activity, toxicity, and conformation of tritrpticin and two TOAC-labeled analogues. Effects on the mechanism of action. Biochim. Biophys. Acta Biomembr. *1862*, 183110.

21. Sungwienwong, I., Ferrie, J.J., Jun, J.V., Liu, C., Barrett, T.M., Hostetler, Z.M., Ieda, N., Hendricks, A., Muthusamy, A.K., Kohli, R.M., et al. (2018). Improving the Fluorescent Probe Acridonylalanine Through a Combination of Theory and Experiment. J. Phys. Org. Chem. *31*, 1–10.

22. Ferrie, J.J., Ieda, N., Haney, C.M., Walters, C.R., Sungwienwong, I., Yoon, J., and Petersson, E.J. (2017). Multicolor protein FRET with tryptophan, selective coumarin-cysteine labeling, and genetic acridonylalanine encoding. Chem. Commun. (Camb.) *53*, 11072–11075.

23. Johnson, W.L., and Straight, A.F. (2013). Fluorescent Protein Applications in Microscopy*Volume 114*, Fourth Edition (Elsevier), pp. 99–123.

24. Erdmann, R.S., Baguley, S.W., Richens, J.H., Wissner, R.F., Xi, Z., Allgeyer, E.S., Zhong, S., Thompson, A.D., Lowe, N., Butler, R., et al. (2019). Labeling Strategies Matter for Super-Resolution Microscopy: A Comparison between HaloTags and SNAP-tags. Cell Chem. Biol. *26*, 584–592.e6.

25. Grimm, J.B., English, B.P., Choi, H., Muthusamy, A.K., Mehl, B.P., Dong, P., Brown, T.A., Lippincott-Schwartz, J., Liu, Z., Lionnet, T., and Lavis, L.D. (2016). Bright photoactivatable fluorophores for single-molecule imaging. Nat. Methods *13*, 985–988.

26. Krasowska, J., Olasek, M., Bzowska, A., Clark, P.L., and Wielgus-Kutrowska, B. (2010). The Comparison of Aggregation and Folding of Enhanced Green Fluorescent Protein (EGFP) by Spectroscopic Studies. Spectroscopy (Springf.) *24*, 343–348.

27. Kubin, R.F., and Fletcher, A.N. (1982). Fluorescence Quantum Yields of Some Rhodamine Dyes. J. Lumin. *27*, 455–462.

28. Kristoffersen, A.S., Erga, S.R., Hamre, B., and Frette, Ø. (2014). Testing fluorescence lifetime standards using two-photon excitation and time-domain instrumentation: rhodamine B, coumarin 6 and lucifer yellow. J. Fluoresc. *24*, 1015–1024.

29. Sjöback, R., Nygren, J., and Kubista, M. (1995). Absorption and Fluorescence Properties of Fluorescein. Spectrochim. Acta Part A Mol. Spectroscopy (Springf.) *51*, L7–L21.

30. Wang, L., Chan, J.Y.W., Rêgo, J.V., Chong, C.M., Ai, N., Falcão, C.B., Rádis-Baptista, G., and Lee, S.M.Y. (2015). Rhodamine B-conjugated encrypted vipericidin nonapeptide is a potent toxin to zebrafish and associated with in vitro cytotoxicity. Biochim. Biophys. Acta *1850*, 1253–1260.

31. El Chamy Maluf, S., Dal Mas, C., Oliveira, E.B., Melo, P.M., Carmona, A.K., Gazarini, M.L., and Hayashi, M.A.F. (2016). Inhibition of malaria parasite Plasmodium falciparum development by crotamine, a cell penetrating peptide from the snake venom. Peptides *78*, 11–16.

32. Chan, J.Y.W., Zhou, H., Kwan, Y.W., Chan, S.W., Radis-Baptista, G., and Lee, S.M.Y. (2017). Evaluation in zebrafish model of the toxicity of rhodamine B-conjugated crotamine, a peptide potentially useful for diagnostics and therapeutics. J. Biochem. Mol. Toxicol. *31*, 1–7.

33. Chileveru, H.R., Lim, S.A., Chairatana, P., Wommack, A.J., Chiang, I.L., and Nolan, E.M. (2015). Visualizing attack of Escherichia coli by the antimicrobial peptide human defensin 5. Biochemistry *54*, 1767–1777.

34. Pant, D., and Girault, H.H. (2005). Time-resolved total internal reflection fluorescence spectroscopy. Part I. Photophysics of Coumarin 343 at liquid/liquid interface. Phys. Chem. Chem. Phys. *7*, 3457–3463.

35. Jun, J.V., Petersson, E.J., and Chenoweth, D.M. (2018). Rational Design and Facile Synthesis of a Highly Tunable Quinoline-Based Fluorescent Small-Molecule Scaffold for Live Cell Imaging. J. Am. Chem. Soc. *140*, 9486–9493.

36. Jun, J.V., Haney, C.M., Karpowicz, R.J., Jr., Giannakoulias, S., Lee, V.M.Y., Petersson, E.J., and Chenoweth, D.M. (2019). A "Clickable" Photoconvertible Small Fluorescent Molecule as a Minimalist Probe for Tracking Individual Biomolecule Complexes. J. Am. Chem. Soc. *141*, 1893–1897.

37. Chen, X., Mietlicki-Baase, E.G., Barrett, T.M., McGrath, L.E., Koch-Laskowski, K., Ferrie, J.J., Hayes, M.R., and Petersson, E.J. (2017). Thioamide Substitution Selectively Modulates Proteolysis and Receptor Activity of Therapeutic Peptide Hormones. J. Am. Chem. Soc. *139*, 16688–16695.

38. Barrett, T.M., Chen, X.S., Liu, C., Giannakoulias, S., Phan, H.A.T., Wang, J., Keenan, E.K., Karpowicz, R.J., Jr., and Petersson, E.J. (2020). Studies of Thioamide Effects on Serine Protease Activity Enable Two-Site Stabilization of Cancer Imaging Peptides. ACS Chem. Biol. *15*, 774–779.

39. Liu, C., Barrett, T.M., Chen, X., Ferrie, J.J., and Petersson, E.J. (2019). Fluorescent Probes for Studying Thioamide Positional Effects on Proteolysis Reveal Insight into Resistance to Cysteine Proteases. ChemBioChem *20*, 2059–2062.

40. Yang, C., Wang, Q., and Ding, W. (2019). Recent Progress in the Imaging Detection of Enzyme Activities in Vivo. RSC Advances *9*, 25285–25302.

41. Choi, J.W., Choi, S.H., Hong, S.T., Kim, M.S., Ryu, S.S., Yoon, Y.U., Paik, K.C., Han, M.S., Sim, T., and Cho, B.R. (2020). Two-photon probes for the endoplasmic reticulum: its detection in a live tissue by two-photon microscopy. Chem. Commun. (Camb.) *56*, 3657–3660.

42. Martinić, I., Eliseeva, S.V., and Petoud, S. (2017). Near-Infrared Emitting Probes for Biological Imaging: Organic Fluorophores, Quantum Dots, Fluorescent Proteins, Lanthanide(III) Complexes and Nanomaterials. J. Lumin. *189*, 19–43.

43. Chen, M., Cheng, K.W., Chen, Y.J., Wang, C.H., Cheng, T.C., Chang, K.C., Kao, A.P., and Chuang, K.H. (2017). Real-time imaging of intestinal bacterial β-glucuronidase activity by hydrolysis of a fluorescent probe. Sci. Rep. *7*, 3142.

44. Jin, Y., Tian, X., Jin, L., Cui, Y., Liu, T., Yu, Z., Huo, X., Cui, J., Sun, C., Wang, C., et al. (2018). Highly Specific near-Infrared Fluorescent Probe for the Real-Time Detection of β-Glucuronidase in Various Living Cells and Animals. Anal. Chem. *90*, 3276–3283.

45. Wu, H., Alexander, S.C., Jin, S., and Devaraj, N.K. (2016). A Bioorthogonal Near-Infrared Fluorogenic Probe for mRNA Detection. J. Am. Chem. Soc. *138*, 11429–11432.

46. Xiong, J., Xia, L., Huang, Q., Huang, J., Gu, Y., and Wang, P. (2018). Cyanine-based NIR fluorescent probe for monitoring H_2S and imaging in living cells and in vivo. Talanta *184*, 109–114.

47. Suseela, Y.V., Narayanaswamy, N., Pratihar, S., and Govindaraju, T. (2018). Far-red fluorescent probes for canonical and non-canonical nucleic acid structures: current progress and future implications. Chem. Soc. Rev. *47*, 1098–1131.

48. Yin, K., Yu, F., Zhang, W., and Chen, L. (2015). A near-infrared ratiometric fluorescent probe for cysteine detection over glutathione indicating mitochondrial oxidative stress in vivo. Biosens. Bioelectron. *74*, 156–164.

49. Narayanaswamy, N., Das, S., Samanta, P.K., Banu, K., Sharma, G.P., Mondal, N., Dhar, S.K., Pati, S.K., and Govindaraju, T. (2015).

Sequence-specific recognition of DNA minor groove by an NIR-fluorescence switch-on probe and its potential applications. Nucleic Acids Res. *43*, 8651–8663.

50. Burggraaf, J., Kamerling, I.M., Gordon, P.B., Schrier, L., de Kam, M.L., Kales, A.J., Bendiksen, R., Indrevoll, B., Bjerke, R.M., Moestue, S.A., et al. (2015). Detection of colorectal polyps in humans using an intravenously administered fluorescent peptide targeted against c-Met. Nat. Med. *21*, 955–961.

51. Joshi, B.P., Zhou, J., Pant, A., Duan, X., Zhou, Q., Kuick, R., Owens, S.R., Appelman, H., and Wang, T.D. (2016). Design and Synthesis of Near-Infrared Peptide for in Vivo Molecular Imaging of HER2. Bioconjug. Chem. *27*, 481–494.

52. Signore, A., Glaudemans, A.W.J.M., Galli, F., and Rouzet, F. (2015). Imaging infection and inflammation. BioMed Res. Int. *2015*, 615150.

53. Ebenhan, T., Chadwick, N., Sathekge, M.M., Govender, P., Govender, T., Kruger, H.G., Marjanovic-Painter, B., and Zeevaart, J.R. (2014). Peptide synthesis, characterization and ^{68}Ga-radiolabeling of NOTA-conjugated ubiquicidin fragments for prospective infection imaging with PET/CT. Nucl. Med. Biol. *41*, 390–400.

54. Ebenhan, T., Zeevaart, J.R., Venter, J.D., Govender, T., Kruger, G.H., Jarvis, N.V., and Sathekge, M.M. (2014). Preclinical evaluation of 68Ga-labeled 1,4,7-triazacyclononane-1,4,7-triacetic acid-ubiquicidin as a radioligand for PET infection imaging. J. Nucl. Med. *55*, 308–314.

55. Vilche, M., Reyes, A.L., Vasilskis, E., Oliver, P., Balter, H., and Engler, H. (2016). ^{68}Ga-NOTA-UBI-29-41 as a PET tracer for detection of bacterial infection. J. Nucl. Med. *57*, 622–627.

56. Bhusari, P., Bhatt, J., Sood, A., Kaur, R., Vatsa, R., Rastogi, A., Mukherjee, A., Dash, A., Mittal, B.R., and Shukla, J. (2019). Evaluating the potential of kit-based 68Ga-ubiquicidin formulation in diagnosis of infection: a pilot study68Ga. Nucl. Med. Commun. *40*, 228–234.

57. Ebenhan, T., Sathekge, M.M., Lengana, T., Koole, M., Gheysens, O., Govender, T., and Zeevaart, J.R. (2018). ^{68}Ga-NOTA-functionalized ubiquicidin: cytotoxicity, biodistribution, radiation dosimetry, and first-in-human PET/CT imaging of infections. J. Nucl. Med. *59*, 334–339.

58. Chen, X., Park, R., Hou, Y., Tohme, M., Shahinian, A.H., Bading, J.R., and Conti, P.S. (2004). microPET and autoradiographic imaging of GRP receptor expression with ^{64}Cu-DOTA-[Lys3]bombesin in human prostate adenocarcinoma xenografts. J. Nucl. Med. *45*, 1390–1397.

59. Mak, I.Y.F., Hayes, A.R., Khoo, B., and Grossman, A. (2019). Peptide Receptor Radionuclide Therapy as a Novel Treatment for Metastatic and Invasive Phaeochromocytoma and Paraganglioma. Neuroendocrinology *109*, 287–298.

60. Strosberg, J., El-Haddad, G., Wolin, E., Hendifar, A., Yao, J., Chasen, B., Mittra, E., Kunz, P.L., Kulke, M.H., Jacene, H., et al.; NETTER-1 Trial Investigators (2017). Phase 3 trial of ^{177}lu-dotatate for midgut neuroendocrine tumors. N. Engl. J. Med. *376*, 125–135.

61. Frilling, A., Weber, F., Saner, F., Bockisch, A., Hofmann, M., Mueller-Brand, J., and Broelsch, C.E. (2006). Treatment with (^{90})Y- and (^{177})Lu-DOTATOC in patients with metastatic neuroendocrine tumors. Surgery *140*, 968–976, discussion 976–977.

62. Strosberg, J., Wolin, E., Chasen, B., Kulke, M., Bushnell, D., Caplin, M., Baum, R.P., Kunz, P., Hobday, T., Hendifar, A., et al.; NETTER-1 Study Group (2018). Health-related quality of life in patients with progressive midgut neuroendocrine tumors treated with ^{177}lu-dotatate in the phase III netter-1 trial. J. Clin. Oncol. *36*, 2578–2584.

63. Emmett, L., Willowson, K., Violet, J., Shin, J., Blanksby, A., and Lee, J. (2017). Lutetium ^{177} PSMA radionuclide therapy for men with prostate cancer: a review of the current literature and discussion of practical aspects of therapy. J. Med. Radiat. Sci. *64*, 52–60.

64. Delker, A., Fendler, W.P., Kratochwil, C., Brunegraf, A., Gosewisch, A., Gildehaus, F.J., Tritschler, S., Stief, C.G., Kopka, K., Haberkorn, U., et al. (2016). Dosimetry for (^{177})Lu-DKFZ-PSMA-617: a new radiopharmaceutical for the treatment of metastatic prostate cancer. Eur. J. Nucl. Med. Mol. Imaging *43*, 42–51.

65. Heck, M.M., Retz, M., D'Alessandria, C., Rauscher, I., Scheidhauer, K., Maurer, T., Storz, E., Janssen, F., Schottelius, M., Wester, H.J., et al. (2016). Systemic Radioligand Therapy with (^{177})Lu Labeled Prostate Specific Membrane Antigen Ligand for Imaging and Therapy in Patients with Metastatic Castration Resistant Prostate Cancer. J. Urol. *196*, 382–391.

66. Ray Banerjee, S., Chen, Z., Pullambhatla, M., Lisok, A., Chen, J., Mease, R.C., and Pomper, M.G. (2016). Preclinical comparative study of ^{68}Ga-labeled DOTA, NOTA, and HBED-CC chelated radiotracers for targeting PSMA. Bioconjug. Chem. *27*, 1447–1455.

67. Liolios, C., Schäfer, M., Haberkorn, U., Eder, M., and Kopka, K. (2016). Novel Bispecific PSMA/GRPr Targeting Radioligands with Optimized Pharmacokinetics for Improved PET Imaging of Prostate Cancer. Bioconjug. Chem. *27*, 737–751.

68. Escudero-Castellanos, A., Ocampo-García, B., Ferro-Flores, G., Santos-Cuevas, C., Morales-Ávila, E., Luna-Gutiérrez, M., and Isaac-Olivé, K. (2019). Synthesis and preclinical evaluation of the ^{177}Lu-DOTA-PSMA(inhibitor)-Lys3-bombesin heterodimer designed as a radiotheranostic probe for prostate cancer. Nucl. Med. Commun. *40*, 278–286.

69. Shi, J., Votruba, A.R., Farokhzad, O.C., and Langer, R. (2010). Nanotechnology in drug delivery and tissue engineering: from discovery to applications. Nano Lett. *10*, 3223–3230.

70. Fan, Z., Sun, L., Huang, Y., Wang, Y., and Zhang, M. (2016). Bioinspired fluorescent dipeptide nanoparticles for targeted cancer cell imaging and real-time monitoring of drug release. Nat. Nanotechnol. *11*, 388–394.

71. Fan, Z., Chang, Y., Cui, C., Sun, L., Wang, D.H., Pan, Z., and Zhang, M. (2018). Near infrared fluorescent peptide nanoparticles for enhancing esophageal cancer therapeutic efficacy. Nat. Commun. *9*, 2605.

72. Mei, J., Leung, N.L.C., Kwok, R.T.K., Lam, J.W.Y., and Tang, B.Z. (2015). Aggregation-Induced Emission: Together We Shine, United We Soar! Chem. Rev. *115*, 11718–11940.

73. Zhao, J., Dong, Z., Cui, H., Jin, H., and Wang, C. (2018). Nanoengineered Peptide-Grafted Hyperbranched Polymers for Killing of Bacteria Monitored in Real Time via Intrinsic Aggregation-Induced Emission. ACS Appl. Mater. Interfaces *10*, 42058–42067.

74. Sun, M., Hong, C.Y., and Pan, C.Y. (2012). A unique aliphatic tertiary amine chromophore: fluorescence, polymer structure, and application in cell imaging. J. Am. Chem. Soc. *134*, 20581–20584.

75. Dwivedi, S., Wahab, R., Khan, F., Mishra, Y.K., Musarrat, J., and Al-Khedhairy, A.A. (2014). Reactive oxygen species mediated bacterial biofilm inhibition via zinc oxide nanoparticles and their statistical determination. PLOS ONE *9*, e111289.

76. Mukherjee, A., Shim, Y., and Myong Song, J. (2016). Quantum dot as probe for disease diagnosis and monitoring. Biotechnol. J. *11*, 31–42.

77. Chen, H., Zhang, M., Li, B., Chen, D., Dong, X., Wang, Y., and Gu, Y. (2015). Versatile antimicrobial peptide-based ZnO quantum dots for in vivo bacteria diagnosis and treatment with high specificity. Biomaterials *53*, 532–544.

78. Zhang, M., Yue, J., Cui, R., Ma, Z., Wan, H., Wang, F., Zhu, S., Zhou, Y., Kuang, Y., Zhong, Y., et al. (2018). Bright quantum dots emitting at :1,600 nm in the NIR-IIb window for deep tissue fluorescence imaging. Proc. Natl. Acad. Sci. USA *115*, 6590–6595.

79. Song, C., Zhong, Y., Jiang, X., Peng, F., Lu, Y., Ji, X., Su, Y., and He, Y. (2015). Peptide-Conjugated Fluorescent Silicon Nanoparticles Enabling Simultaneous Tracking and Specific Destruction of Cancer Cells. Anal. Chem. *87*, 6718–6723.

80. Mohid, S.A., Ghorai, A., Ilyas, H., Mroue, K.H., Narayanan, G., Sarkar, A., Ray, S.K., Biswas, K., Bera, A.K., Malmsten, M., et al. (2019). Application of tungsten disulfide quantum dot-conjugated antimicrobial peptides in bio-imaging and antimicrobial therapy. Colloids Surf. B Biointerfaces *176*, 360–370.

81. Galdiero, E., Siciliano, A., Maselli, V., Gesuele, R., Guida, M., Fulgione, D., Galdiero, S., Lombardi, L., and Falanga, A. (2016). An integrated study on antimicrobial activity and ecotoxicity of quantum dots and quantum dots coated with the antimicrobial peptide indolicidin. Int. J. Nanomedicine *11*, 4199–4211.

82. Vacher, M., Fdez Galván, I., Ding, B.W., Schramm, S., Berraud-Pache, R., Naumov, P., Ferré, N., Liu, Y.J., Navizet, I., Roca-Sanjuán, D., et al. (2018). Chemi- and Bioluminescence of Cyclic Peroxides. Chem. Rev. *118*, 6927–6974.

83. Karimzadeh, A., Hasanzadeh, M., Shadjou, N., and de la Guardia, M. (2018). Peptide based biosensors. TrAC Trends Analyt. Chem. *107*, 1–20.

84. Marquette, C.A., and Blum, L.J. (2008). Electro-chemiluminescent biosensing. Anal. Bioanal. Chem. *390*, 155–168.

85. Pu, K., and Huang, J. (2020). Activatable Molecular Probes for Second Near-Infrared Fluorescence, Chemiluminescence, and Photoacoustic Imaging. Angew. Chem. *132*, 2–17.

86. Gnaim, S., and Shabat, D. (2019). Activity-Based Optical Sensing Enabled by Self-Immolative Scaffolds: Monitoring of Release Events by Fluorescence or Chemiluminescence Output. Acc. Chem. Res. *52*, 2806–2817.

87. Gnaim, S., Scomparin, A., Das, S., Blau, R., Satchi-Fainaro, R., and Shabat, D. (2018). Direct Real-Time Monitoring of Prodrug Activation by Chemiluminescence. Angew. Chem. Int. Ed. Engl. *57*, 9033–9037.

88. Schaap, A.P., Handley, R.S., and Giri, B.P. (1987). Chemical and enzymatic triggering of 1,2-dioxetanes. 1: Aryl esterase-catalyzed chemiluminescence from a naphthyl acetate-substituted dioxetane. Tetrahedron Lett. *28*, 935–938.

89. Richard, J.A., Jean, L., Schenkels, C., Massonneau, M., Romieu, A., and Renard, P.Y. (2009). Self-cleavable chemiluminescent probes suitable for protease sensing. Org. Biomol. Chem. *7*, 2941–2957.

90. Li, Y. (2012). Chemiluminescent determination of the activity of caspase-3 using a specific peptide substrate and magnetic beads. Mikrochim. Acta *177*, 443–447.

91. Wu, Y., and Nie, F. (2015). Caspase-1 assay based on peptide and luminol labeled gold nanoparticle as chemiluminescence probe coupling magnetic separation technology. Sens. Actuators B Chem. *220*, 481–484.

92. Cheng, P., Miao, Q., Li, J., Huang, J., Xie, C., and Pu, K. (2019). Unimolecular Chemo-fluoro-luminescent Reporter for Crosstalk-Free Duplex Imaging of Hepatotoxicity. J. Am. Chem. Soc. *141*, 10581–10584.

93. Hu, J.J., Wong, N.K., Ye, S., Chen, X., Lu, M.Y., Zhao, A.Q., Guo, Y., Ma, A.C., Leung, A.Y., Shen, J., and Yang, D. (2015). Fluorescent Probe HKSOX-1 for imaging and detection of endogenous superoxide in live cells and in vivo. J. Am. Chem. Soc. *137*, 6837–6843.

94. Jones, L.R., Goun, E.A., Shinde, R., Rothbard, J.B., Contag, C.H., and Wender, P.A. (2006). Releasable luciferin-transporter conjugates: tools for the real-time analysis of cellular uptake and release. J. Am. Chem. Soc. *128*, 6526–6527.

95. Eiríksdóttir, E., Mäger, I., Lehto, T., El Andaloussi, S., and Langel, U. (2010). Cellular internalization kinetics of (luciferin-)cell-penetrating peptide conjugates. Bioconjug. Chem. *21*, 1662–1672.

96. Poutiainen, P.K., Rönkkö, T., Hinkkanen, A.E., Palvimo, J.J., Närvänen, A., Turhanen, P., Laatikainen, R., Weisell, J., and Pulkkinen, J.T. (2014). Firefly luciferase inhibitor-conjugated peptide quenches bioluminescence: a versatile tool for real time monitoring cellular uptake of biomolecules. Bioconjug. Chem. *25*, 4–10.

97. Karatas, H., Maric, T., D'Alessandro, P.L., Yevtodiyenko, A., Vorherr, T., Hollingworth, G.J., and Goun, E.A. (2019). Real-Time Imaging and Quantification of Peptide Uptake *in Vitro* and *in Vivo*. ACS Chem. Biol. *14*, 2197–2205.